

Application of GRU Network-Based UWB Localization Algorithm for Indoor Robot Localization

Fangyong Hu¹, Lanshuai Lou¹, and Wenbo Ma²

¹ School of Information and Control Engineering, Jilin Institute of Chemical Technology, Jilin 132000, China

² School of Computer and Information, Dezhou University, Dezhou 253000, China

Abstract

In indoor mobile robot localization systems based on ultra-wideband (UWB) technology, nonlinear noise caused by non-line-of-sight (NLOS) environments severely limits positioning performance. We propose a gated recurrent unit (GRU) network-based ranging error mitigation method to enhance mobile robot localization in nonlinear noise scenarios. The model is optimized with early stopping, and the corrected ranging are applied to least squares localization. The experimental results show that: the proposed localization model reduces the mean absolute error (MAE) by at least 29.12% and the root mean square error (RMSE) by at least 32.3% compared to the error mitigation method based on the long short-term memory (LSTM) network, and the localization accuracy is significantly improved.

Keywords

Mobile Robot; NLOS; GRU; Nonlinearity; Ranging Error Mitigation.

1. Introduction

With the advent of the automation era, robotics is rapidly developing. Mobile robots are widely used in hazardous exploration [1], cargo handling [2], and industrial inspection [3], etc. Accurate and robust localization is a prerequisite for mobile robots to achieve navigation and path planning and is one of the research hotspots in the field of robotics [4]. Although mature satellite localization systems such as the global localization system (GPS) and the beidou navigation satellite system (BDS) are widely used in outdoor environments, indoor obstructions like walls weaken their signals and lead to unreliable robot localization. Therefore, the issue of high-precision indoor localization for robots still needs further resolution. Many researchers have proposed indoor localization technologies such as UWB, ultrasound, infrared, Bluetooth, ZigBee, radio frequency identification (RFID), and wi-fi to meet high-precision indoor localization demands [5]. However, these traditional methods are prone to environmental interference and limited in accuracy. Recently, UWB has shown potential for high-precision indoor localization due to its high spatiotemporal resolution, low power consumption, and strong penetration [6]. However, the indoor NLOS effect makes it difficult or even impossible to localize the UWB localization system in nonlinear noise [7]. Therefore, effective error mitigation is crucial to improving UWB localization accuracy.

Currently, many researchers have proposed methods to address reduced localization accuracy in NLOS environments. These methods fall into categories such as regression, weighting, filtering, and neural networks [8]. Yang X [9] introduced an improved sparse pseudorange input gaussian process by modeling ranging error as a gaussian regression model, which offers low computational complexity and effective error mitigation. The weighted localization method uses all available measurements and assigns weighting factors to residuals based on measurement characteristics to reduce NLOS

error impact. Wei J et al. [10] applied a minimum residual weighting method to recalibrate Chan algorithm localization estimates and used this as the initial value for Newton's method to enhance accuracy. Zhang Y et al. [11] proposed using higher powers of residuals as weighting functions to further improve localization accuracy. While weighting algorithms improve localization performance, they depend heavily on a priori information and optimal weight selection is challenging. Researchers have therefore turned to innovative filtering algorithms to effectively mitigate NLOS error and enhance localization accuracy in UWB systems. Liu Y R et al. [12] proposed an improved particle filtering localization algorithm that uses the Kalman filter to construct an importance probability density function, addressing particle degradation and aligning particle distribution with the posterior probability distribution. This algorithm improves localization accuracy in both LOS and NLOS environments but struggles with frequently changing measurement noise. To address this, Gao Y et al. [13] proposed a volumetric Kalman filter parameter adaptive localization algorithm, which uses the sigmoid function to update the observation noise matrix in real-time, enhancing system stability and localization accuracy through dynamic trajectory correction in NLOS environments. In recent years, deep learning has been applied to the UWB localization field due to its powerful feature extraction capabilities, nonlinear modeling capabilities, and ability to handle large-scale data. Poulouse A et al. [14] used two LSTM networks to predict tag localizations using time of arrival (TOA) ranging information and analyzed the performance of the LSTM model in terms of learning rate, optimizer, loss function and batch size. The results show that this method has higher localization accuracy compared to traditional localization methods. Differently, Han D S et al. [15] further improved the feature extraction capability of the LSTM network by extracting the maximum, minimum, 25th, 50th, and 75th percentiles of the ranging data from the raw time of arrival (TOA) ranging information and inputting them into deep long short-term memory (DLSTM) networks to predict tag localizations, ultimately achieving an average localization error of 5 cm. To optimize the ranging, researchers have mitigated ranging errors by inputting extracted characteristics of the original channel impulse response (CIR) signals into (deep neural networks) DNN [16], (convolutional neural network) CNN and LSTM [17], which improves localization performance but also comes with high computational complexity. Li C et al. [18] proposed directly inputting ranging into the LSTM network for ranging error mitigation, and the final results show that the proposed method can effectively improve localization accuracy. The aforementioned deep neural network-based UWB localization algorithms outperform traditional methods without prior knowledge but incur high computational costs due to model complexity.

In summary, most UWB-based NLOS mitigation methods, like gaussian regression models [9] and weighted localization algorithms [10][11], depend on known statistical error properties and struggle with strong nonlinearities. Deep learning approaches using CIR signal characteristics [16][17] face high model complexity. Therefore, this paper proposes a new least squares localization method using GRU-optimized ranging to enhance mobile robot localization in strongly nonlinear noise environments.

2. UWB-based Indoor Localization Model

2.1 UWB Ranging Model

The ADS-TWR scheme proposed in [19] is selected for indoor robot localization to reduce errors from clock and frequency drift compared to the basic DS-TWR scheme, focusing on antenna delay effects. The ranging protocol is illustrated in Figures 1 and 2, with the associated time of fly (TOF) expressions provided.

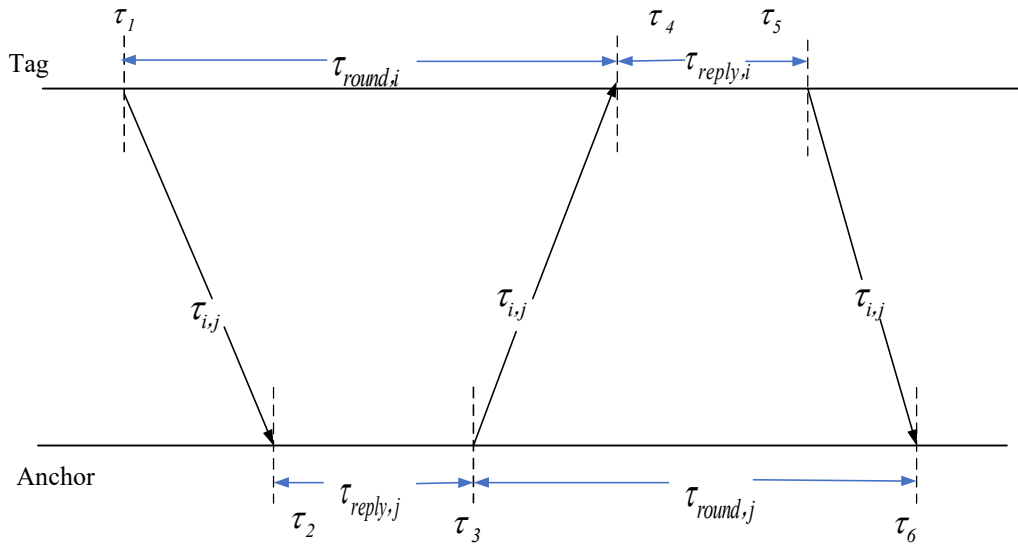


Fig. 1 DS-TWR ranging model

Let the first round-trip time starting from the tag be: $\tau_{round,i} = \tau_4 - \tau_1 = 2\tau_{i,j} + \tau_{reply,j}$. Similarly, on the anchor side: $\tau_{round,j} = \tau_6 - \tau_3 = 2\tau_{i,j} + \tau_{reply,i}$. Here $\tau_{reply,i}$ and $\tau_{reply,j}$ are the reply times of the tag and the anchor, respectively. The flight time is then expressed as:

$$\tau_{i,j} = \frac{\tau_{round,i}\tau_{round,j} - \tau_{reply,i}\tau_{reply,j}}{\tau_{reply,j} + \tau_{reply,i} + \tau_{round,i} + \tau_{round,j}} \quad (1)$$

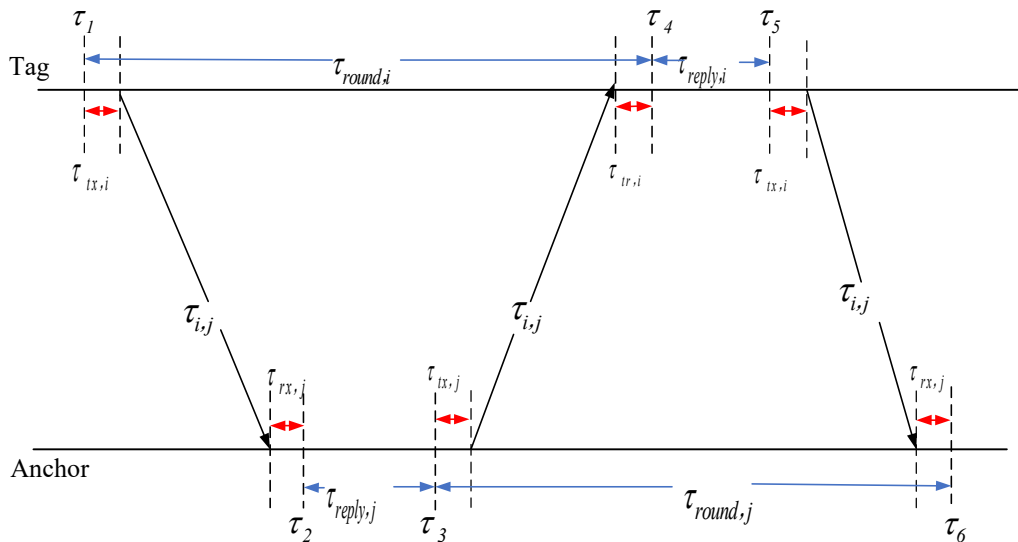


Fig. 2 ADS-TWR ranging model considering antenna delay

The above equations assume ideal conditions without additional hardware-induced antenna delays between the transmitter and receiver. Considering the antenna delays at both the transmitter and receiver ends, we derive: $\tau_{round,i} = \tau_4 - \tau_1 = 2\tau_{i,j} + \tau_{reply,j} + \tau_{AD,i,j}$, $\tau_{round,j} = \tau_6 - \tau_3 = 2\tau_{i,j} + \tau_{reply,i} + \tau_{AD,i,j}$. The total antenna delay is given by: $\tau_{AD,i,j} = \tau_{tx,i} + \tau_{rx,i} + \tau_{tx,j} + \tau_{rx,j}$. Therefore, the flight time is re-expressed as:

$$\tau_{i,j}(\tau_{AD,i,j}) = \frac{\tau_{round,i}\tau_{round,j} - (\tau_{reply,i}\tau_{reply,j})\tau_{AD,i,j} - \tau_{AD,i,j}^2}{\tau_{reply,j} + \tau_{reply,j} + \tau_{round,i} + \tau_{round,i} + 2\tau_{AD,i,j}} \quad (2)$$

Therefore, the ranging error model constructed in this paper is:

$$d_n = d_m - d_q \quad (3)$$

Where d_q is the euclidean distance between the base station and the robot localization tag, d_n is the ranging error, $d_m = c \times \tau_{i,j}(\tau_{AD,i,j})$ is the measured distance, and c is the s-speed of light.

2.2 Least Squares Localization Method based on Optimized Ranging

Using the above ranging error mitigation method, the distance from each base station to the robot tag, d_p , is obtained. The coordinates of the N base stations are known as (x_1, y_1) , $(x_2, y_2), \dots, (x_N, y_N)$. The system of equations can be formulated as follows:

$$\begin{cases} d_1 = \sqrt{(x_1 - x)^2 + (y_1 - y)^2} \\ \vdots \\ d_N = \sqrt{(x_N - x)^2 + (y_N - y)^2} \end{cases} \quad (4)$$

where $p \in (1, N)$ and (x, y) are the coordinates of the robot to be localized. The computation uses the least squares method, with the first $N - 1$ equations subtracted from the N -th equation to obtain the linearized equation: $AX = b$, where:

$$A = \begin{bmatrix} 2(x_1 - x_N) & 2(y_1 - y_N) \\ \vdots & \vdots \\ 2(x_{N-1} - x_N) & 2(y_{N-1} - y_N) \end{bmatrix} \quad (5)$$

$$b = \begin{bmatrix} x_1^2 - x_N^2 + y_1^2 - y_N^2 + d_N^2 - d_1^2 \\ \vdots \\ x_{N-1}^2 - x_N^2 + y_{N-1}^2 - y_N^2 + d_N^2 - d_{N-1}^2 \end{bmatrix} \quad (6)$$

Finally, by employing the least mean squares method, we derive the following solution:

$$X = \begin{bmatrix} x \\ y \end{bmatrix} = (A^T A)^{-1} A^T b \quad (7)$$

The optimized ranging are then applied to least squares localization to determine the robot's coordinates, achieving the optimal solution by minimizing the mean error between the actual and calculated coordinates.

3. Error Mitigation Model based on GRU Network

3.1 GRU Network Structure

Due to the continuity and correlation of ranging errors over time in robot localization, the ranging optimization method in this paper is treated as a time series prediction problem. LSTM is superior for addressing gradient explosion and vanishing issues in RNNs when learning long-term dependencies [20][21]. As a simplified version of LSTM, GRU offers higher efficiency in capturing long-term dependencies and reduces modeling complexity and computational cost. Thus, the GRU network model is chosen for optimizing ranging in the robot localization process. The internal structure of the neural network is shown in Fig. 3, with related expressions as follows.

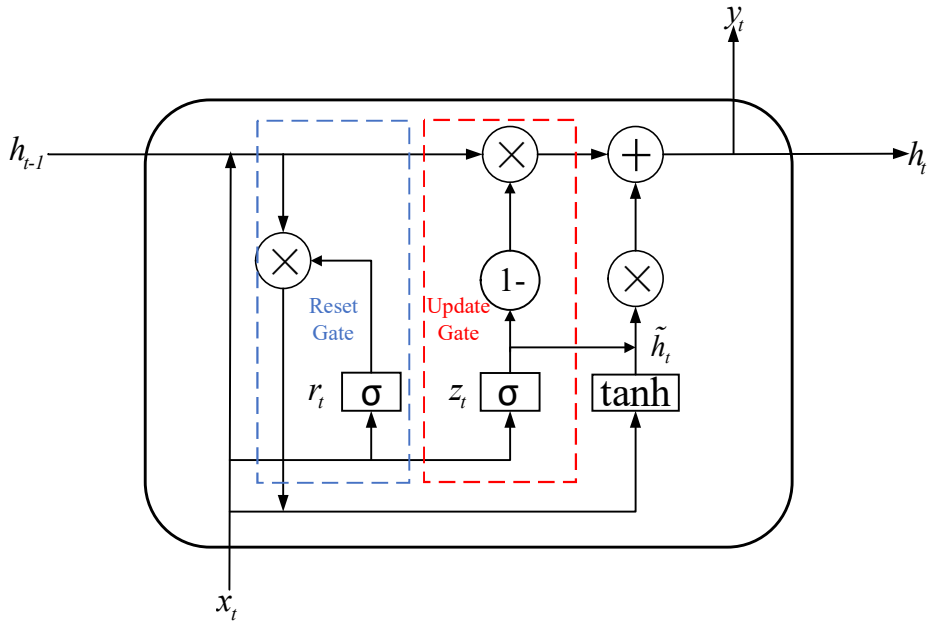


Fig. 3 Basic GRU unit

$$z_t = \sigma(\omega_z \cdot [h_{t-1}, x_t]) \quad (8)$$

The role of the update gate z_t is to determine to what extent the previous moment's robot ranging state h_{t-1} is introduced into the current moment's robot ranging state h_t .

$$r_t = \sigma(\omega_r \cdot [h_{t-1}, x_t]) \quad (9)$$

The role of the reset gate r_t is to control the extent to which the previous moment's state of the robot ranging h_{t-1} affects the candidate \tilde{h}_t hiding state.

$$\tilde{h}_t = \phi(\omega_{\tilde{h}} \cdot [r_t \times h_{t-1}, x_t]) \quad (10)$$

The candidate hidden state \tilde{h}_t is computed from the previous moment's robot ranging state $r_t \times h_{t-1}$ after reset and the current input x_t .

$$h_t = (1 - z_t) \times h_{t-1} + z_t \times \tilde{h}_t \quad (11)$$

The final hidden state h_t combines the previous moment's robot ranging state h_{t-1} and the current candidate hidden state \tilde{h}_t , whose proportions are controlled by the update gate z_t .

$$y_t = \sigma(\omega_o \cdot h_t) \quad (12)$$

Finally, output the robot ranging $y_t = [d_{q,1}, d_{q,2}, d_{q,3}, d_{q,4}, d_{q,5}, d_{q,6}, d_{q,7}, d_{q,8}]$.

In Figure 3 and the above equations, $x_t = [d_{m,1}, d_{m,2}, d_{m,3}, d_{m,4}, d_{m,5}, d_{m,6}, d_{m,7}, d_{m,8}]$, h_{t-1} , h_t , r_t , z_t , \tilde{h}_t , $y_t = [d_{q,1}, d_{q,2}, d_{q,3}, d_{q,4}, d_{q,5}, d_{q,6}, d_{q,7}, d_{q,8}]$ represent the input vector, the state memory variable at the previous time step, the state memory variable at the current time step, the

update gate state, the reset gate state, the state of the current candidate set, and the output vector at the current time step, respectively. ω_r , ω_z , $\omega_{\tilde{h}}$, ω_o are the weight parameters of the connection matrices corresponding to the reset gate, update gate, candidate state, and output vector, respectively. I represents the identity matrix, $[]$ represents the concatenation of vectors, \cdot represents the matrix dot product, \times represents matrix multiplication, σ denotes the sigmoid activation function, and \emptyset represents the tanh activation function. The mathematical expressions for σ and \emptyset are as follows:

$$\sigma(x) = \frac{1}{1 + e^{-x}} \quad (13)$$

$$\emptyset(x) = \tanh(x) = \frac{e^x - e^{-x}}{e^x + e^{-x}} \quad (14)$$

The core modules of the GRU are the update gate and the reset gate. The concatenated matrix of the input variable x_t and the previous state memory variable h_{t-1} undergoes a *sigmoid* nonlinear transformation before being fed into the update gate, which determines the extent to which the previous state influences the current state. The reset gate controls the amount of information from the previous state that can be written into the candidate set. The previous state's information is preserved through $(I - z_t) \times h_{t-1}$, while the current state's information is recorded through $z_t \times \tilde{h}_t$. The sum of these two components constitutes the output at the current time step. In indoor UWB-based robot localization, obstacles cause the ranging error between the robot tag and base station to exhibit strong nonlinear and non-gaussian characteristics [22]. This paper employs a GRU recurrent neural network for ranging error mitigation. The GRU model is optimized using the Nadam optimizer and Huber loss function, with an early stopping function to prevent overfitting. The pseudo-code for the error mitigation algorithm is as follows.

Algorithm 1: Ranging error mitigation model based on GRU

Input: Training dataset D , testing dataset K , validation dataset V

Output: Optimal weights ω

Initialize network weights ω , learning rate η and other parameters;

Compile the model using the Nadam optimizer and Huber loss function, and apply early stopping for optimization;

return optimal weights ω

3.2 Loss Function based on Early Stopping Function

When training the GRU network, the gradient descent algorithm optimizes model performance by updating parameters to minimize the loss function. The Nadam optimizer, which combines the advantages of Nesterov momentum and Adam[23], updates the model parameters as follows.

$$m_t = \beta_1 m_{t-1} + (1 - \beta_1) g_t \quad (15)$$

$$v_t = \beta_2 v_{t-1} + (1 - \beta_2) g_t^2 \quad (16)$$

$$\hat{m}_t = \frac{m_t}{1 - \beta_1^t} \quad (17)$$

$$\hat{v}_t = \frac{v_t}{1 - \beta_2^t} \quad (18)$$

$$n_t = \beta_1 \hat{m}_t + \frac{1 - \beta_1}{1 - \beta_1^t} \quad (19)$$

$$\theta_{t+1} = \theta_t - \frac{\eta n_t}{\sqrt{\hat{v}_t + \epsilon}} \quad (20)$$

where, g_t is the gradient of the loss function with respect to the model p-parameters at time step t , m_t and v_t are the first-order and second-order moment-um estimates, β_1 and β_2 are the first-order and second-order momentum decay coefficients, \hat{m}_t and \hat{v}_t are the bias corrected first-order and second-order mo-mentum estimates, respectively, n_t is the Nest-erov gradient, η is the learning rate, ϵ is the constant used to ensure the numerical stabi-lity, and θ_t are the mod-el parameters. The Nesterov-accelerated adaptive moment estimation optimizer u-pdates the model parameters in such a way that it converges to the optimal s-olution faster than conventional optimization methods.

To prevent overfitting, an early stop function is introduced to monitor the loss on the validation set. The training loss $L_1(t)$ and the validation loss $L_2(t)$ are computed for each training cycle t :

$$Huber(d_q, d_p) = \begin{cases} \frac{1}{2}(d_q - d_p)^2, & |d_q - d_p| \leq \delta \\ \delta \cdot |d_q - d_p| - \frac{1}{2}\delta^2, & |d_q - d_p| > \delta \end{cases} \quad (21)$$

$$L_1(t) = \frac{1}{N} \sum_{i=1}^N Huber(d_{q,i}, d_{p,i}) \quad (22)$$

$$L_2(t) = \frac{1}{M} \sum_{j=1}^M Huber(d_{q,j}, d_{p,j}) \quad (23)$$

Check if the validation loss improves in p cycles, if it does not improve in p cycles then stop training early.

$$L_1(t) \geq \min\{L_2(t - p), L_2(t - p + 1), \dots, L_2(t - 1)\} \quad (24)$$

Where $d_{l,i}$ and $d_{p,i}$ are the true and predicted ranging of the i -th training sa-mples in the robot localization process, $d_{l,j}$ and $d_{p,j}$ are the true and predicted ranging val-ues of the j -th validation sample in the robot localization process, N is the number of training sa-mples, and M is the number of validation samples.

4. Test Results and Analysis

4.1 Analysis of Data Sets

To validate the performance of the method, this paper uses the public dataset from Klemen Bregar [24]. The test includes 21,080 ranging samples, divided into 80% for training the GRU model (with 10% of this as the validation set to prevent overfitting) and 20% for testing. After data processing, the localization performance of several methods is compared. The test setup includes an AMD R9-7945HX processor, 16GB RAM, Python 3.8.19, and TensorFlow 2.13.0. Error curves of the measured distances from each base station to the tag, based on the ADS-TWR protocol, are shown in Fig. 4.

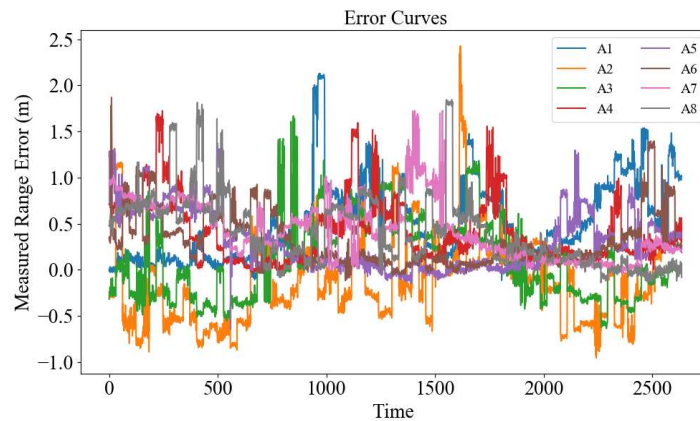


Fig. 4 Error curves of measured ranging for each base station

4.2 GRU Model Optimization for NLOS Error Mitigation

The GRU model is trained using an optimizer and loss function on a dataset of true ranging and corresponding erroneous data from robot localization. The model adjusts its weights to minimize the loss function, choosing optimizer and loss function crucial for effective training.

As deep neural network parameters increase, gradient vanishing and explosion problems can affect performance. To avoid these, a suitable optimizer is essential. During training and validation, the performance of stochastic gradient descent (SGD), adaptive moment estimation (Adam), Adam optimizer based on infinite paradigms (Adamax), adaptive gradient algorithm (Adagrad), nesterov-accelerated adaptive moment estimation (Nadam) was analyzed. The Nadam optimizer was ultimately chosen for its fast convergence, good stability, and lower loss on both training and validation sets. Performance comparisons are shown in Figs 5 and 6.

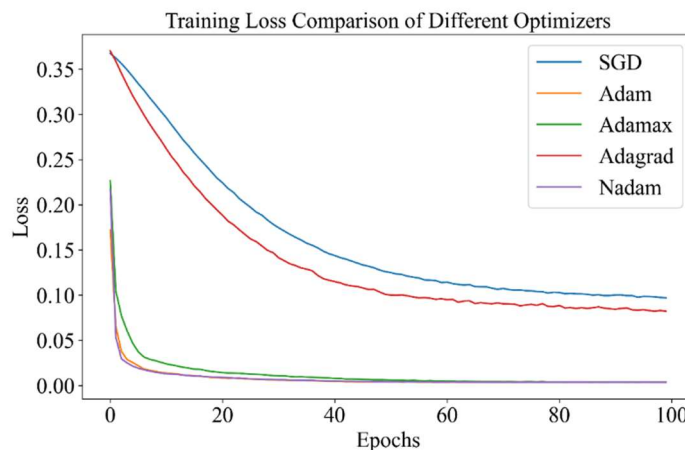


Fig. 5 Training loss for different optimizers

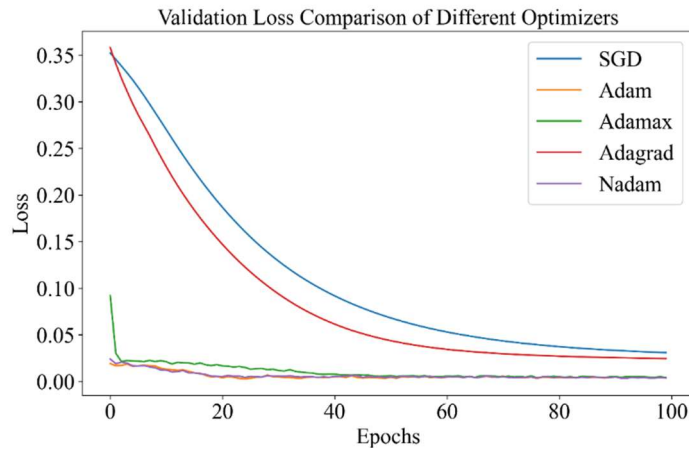


Fig. 6 Validation loss for different optimizers

The choice of loss function in deep learning models is crucial for reducing prediction errors. For regression models, mean squared error (MSE), Huber loss, and MAE are commonly used. After experimental analysis, Huber loss was selected for its lowest loss values, stability during training and validation, and robustness to outliers. Performance comparisons are shown in Figs 7 and 8.

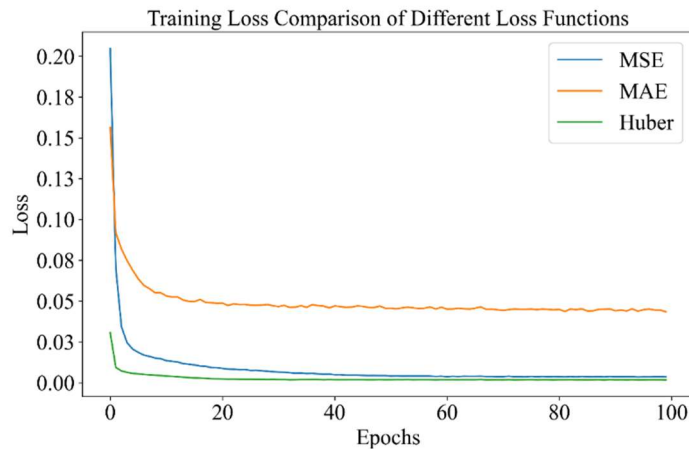


Fig. 7 Training loss for different loss functions

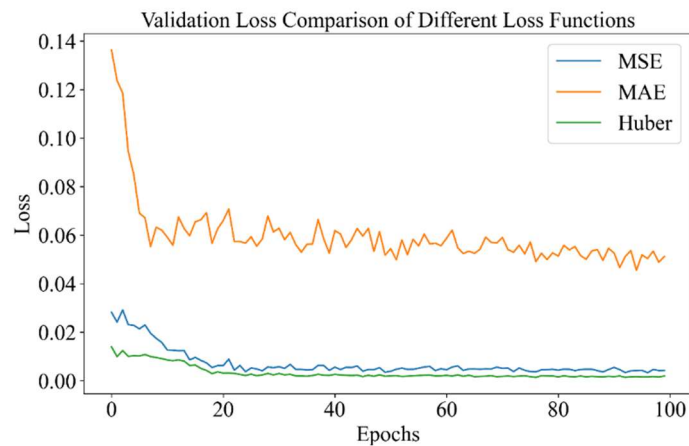


Fig. 8 Validation loss for different loss functions

To prevent overfitting, an early stopping function monitors validation loss and halts training when it no longer improves. This ensures optimal generalization while saving time and computational resources. The training and validation losses after deploying the early stopping function are shown in Fig. 9.

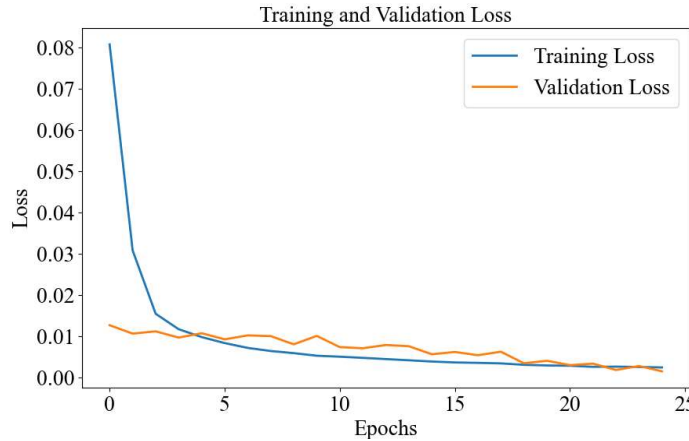


Fig. 9 Training and validation loss

Fig. 9 shows the training and validation losses over 25 epochs. The losses converge as epochs increase. When performance on the validation set stops improving or declines, the model is considered to be overfitting, and the early stopping mechanism is triggered.

4.3 Comparison of Localization Results

To verify the localization algorithm's performance, this paper compares the gaussian process regression (GPR)-based method [9], the LSTM-based ranging error mitigation method [18], and the improved GRU model with early stopping proposed here. MAE and RMSE are used as evaluation metrics. The specific error calculations are as follows.

$$MAE = \frac{1}{n} \sum_{i=1}^n \sqrt{(\hat{x}_i - x_i)^2 + (\hat{y}_i - y_i)^2} \quad (25)$$

$$RMSE = \sqrt{\frac{1}{n} \sum_{i=1}^n [(\hat{x}_i - x_i)^2 + (\hat{y}_i - y_i)^2]} \quad (26)$$

Where \hat{x}_i, \hat{y}_i are the robot solved coordinates of the i th sample, and x_i, y_i are the robot real coordinates of the i -th sample. Considering that there are more outliers in the original dataset, the RANSAC algorithm is added to the traditional GPR model to process the outliers and then the kernel function is used to capture the ranging error for the ranging correction, and finally combined with the weighted least squares method for solving the tag localization, and the results of the comparison of several methods are shown in the table below.

The table shows that even with outlier processing, the traditional GPR method struggles with complex nonlinear problems. In contrast, LSTM and GRU models handle time series data better. The improved GRU model, despite increasing localization time by 0.247 milliseconds compared to the method in

literature [18], reduces the MAE by 29.12% and the RMSE by 32.3%, significantly improving the localization performance for indoor mobile robots.

Table 1. Comparison of Localization Performance

Method	MAE/m	RMSE/m	Train time/s	Localization time /ms
GPR	0.219	0.295	/	/
LSTM	0.182	0.226	15.26	0.778
Methodology of this paper	0.129	0.153	9.08	1.025

5. Conclusion

In UWB indoor localization systems, the presence of NLOS poses significant challenges in achieving high-accuracy localization of robotic systems. Traditional error mitigation methods fall short with highly nonlinear systems. To address this, we adopt a deep learning approach, leveraging the GRU model to learn and mitigate ranging noise errors. Experimental results show that the proposed method effectively improves localization performance in mobile robot scenarios with strong nonlinear noise.

References

- [1] D Topolsky, I Topolskaya, I Plaksina, P Shaburov, N Yumagulov, D Fedorov and E Zvereva, Development of a Mobile Robot for Mine Exploration, Processes.2022, 10(5), 865.
- [2] A Bolu and Ö Korçak, Adaptive Task Planning for Multi-Robot Smart Warehouse, IEEE Access.2021, 9,27346-27358.
- [3] X Wang, X Ma and Z Li, Research on SLAM and path planning method of inspection robot in complex scenarios[J], Electronics.2023,12(10),2178.
- [4] J Huang, S Junginger, H Liu and K Thurow, Indoor Localization Systems of Mobile Robots, A Review, Robotics.2023,12(2),47.
- [5] N El-Sheimy and Y Li, Indoor navigation: state of the art and future trends, Satellite Navigation. 2021, 2(1),7.
- [6] GM Mendoza-Silva, J Torres-Sospedra and J Huerta, A Meta-Review of Indoor Localization Systems. Sensors.2019;19(20):4507.
- [7] C De Cock, E Tanghe, W Joseph and D Plets, Robust IMU-Based Mitigation of Human Body Shadowing in UWB Indoor Localization, Sensors.2023,23(19),8289.
- [8] F Wang, H Tang and J Chen, Survey on NLOS Identification and Error Mitigation for UWB Indoor Localization, Electronics.2023,12(7),1678.
- [9] V Barral, C J Escudero, J A García-Naya and R Maneiro-Catoira, NLOS Identification and Mitigation Using Low-Cost UWB Devices, Sensors.2019,19(16),3464.
- [10] J Wei, Z Deng, H Wang, X Zheng, X Fu, and Q Liu, An Improved Chan/Newton Combined Localization Estimate Algorithm. China Satellite Navigation Conference (CSNC).2020,3,437-447.
- [11] Y Zhang, F Shen, Q Liu and W Li, A UWB 3D Localization Algorithm Based on Residual Weighting, IEEE International Conference on Mechatronics and Automation (ICMA).2020,309-313.
- [12] Y. Liu, H Fengqing and J He, A Particle Filter-Based Ultra-Wideband Indoor Localization Optimization Algorithm, Computing and Intelligent Systems (CCIS), 2023, 277-283.
- [13] Y Lv, S Liu, Y Gao, J Dai, Z Ren and Y Liu, An Ultra-Wideband Indoor Localization Algorithm with Improved Cubature Kalman Filtering Based on Sigmoid Function, Applied Sciences.2024,14(6),2239.
- [14] A Poulouse and D S Han, UWB Indoor Localization Using Deep Learning LSTM Networks, Applied Sciences.2020,10(18),6290.

- [15] A Poulouse and D S Han, Feature-Based Deep LSTM Network for Indoor Localization Using UWB Measurements, The 3rd International Conference on Artificial Intelligence in Information and Communication (ICAIIIC).2021,298-301.
- [16] S Angarano, V Mazzia, F Salvetti, G Fantin, and M Chiaberge, Robust ultra-wideband range error mitigation with deep learning at the edge, Engineering Applications of Artificial Intelligence.2021,102, 104278.
- [17] Y Y Chen, S P Huang, T W Wu, W T Tsai, C Y Liou, S G Mao, UWB System for Indoor Localization and Tracking With Arbitrary Target Orientation, Optimal Anchor Location, and Adaptive NLOS Mitigation, IEEE Transactions on Vehicular Technology.2020,69(9),9304-9314.
- [18] C Li, Y Zhang, J Qiao, R Gao, K Liu and Y Zhang, LSTM-Based Error Correction for Reducing UWB Measurement Errors, Proceedings of the 13th International Conference on Computer Engineering and Networks (CENet 2023), Lecture Notes in Electrical Engineering. vol. 1126, Springer, 2024.
- [19] K Bregar, Indoor UWB Localization and Localization Tracking Data Set, Scientific Data.2023, 10(1),744.
- [20] H S Gill, O I Khalaf, Y Alotaibi, S Alghamdi and F Alassery, Multi-Model CNN-RNN-LSTM Based Fruit Recognition and Classification[J], Intelligent Automation & Soft Computing, 2022, 33(1),256.
- [21] M Abumohsen, A Y Owda and M Owda, Electrical load forecasting using LSTM, GRU, and RNN algorithms, Energies.2023,16(5),2283.
- [22] H Zhang, Q Wang, C Yan and B Zhang, Research on UWB Indoor Localization Algorithm under the Influence of Human Occlusion and Spatial NLOS, Remote Sensing.2022,14(24),6338.
- [23] E C Seyrek and M Uysal, A comparative analysis of various activation functions and optimizers in a convolutional neural network for hyperspectral image classification, Multimedia Tools and Applications. 2024,83(18),53785-53816.